This is the accepted manuscript made available via CHORUS. The article has been published as:

Superconductivity enhanced by pair fluctuations between wide and narrow bands

Changming Yue, Hideo Aoki, and Philipp Werner

Phys. Rev. B **106**, L180506 — Published 21 November 2022

DOI: 10.1103/PhysRevB.106.L180506

Superconductivity enhanced by pair fluctuations between wide and narrow bands

Changming Yue,[1,*] Hideo Aoki,[2,3] and Philipp Werner[1,†]

[1] *Department of Physics, University of Fribourg, 1700 Fribourg, Switzerland*
[2] *Department of Physics, University of Tokyo, Hongo, Tokyo 113-0033, Japan*
[3] *Electronics and Photonics Research Institute, National Institute of Advanced Industrial Science and Technology (AIST), Tsukuba 305-8568, Japan*

Full or empty narrow bands near the Fermi level are known to enhance superconductivity by promoting scattering processes and spin fluctuations. Here, we demonstrate that doublon-holon fluctuations in systems with half-filled narrow bands can similarly boost the superconducting T_c. We study the half-filled attractive bilayer Hubbard model on the square lattice using dynamical mean-field theory. The band structure of the noninteracting system contains a wide band formed by bonding orbitals and a narrow band formed by antibonding orbitals, with bandwidths tunable by the inter-layer hopping. The shrinking of the narrow band can lead to a substantial increase in the superconducting order parameter and phase stiffness in the wide band. At the same time, the coupling to the wide band allows the narrow band to remain superconducting – and to reach the largest order parameter – in the flat band limit. We develop an anomalous worm sampling method to study superconductivity in the limit of vanishing effective hopping. By analyzing the histogram of the local eigenstates, we clarify how the interplay between different interaction terms in the bonding/antibonding basis promotes pair fluctuations and superconductivity.

Introduction. Superconductivity in strongly-correlated *multi-band* systems has attracted much interest since the discovery of iron based superconductors [1–14] and also in connection with twisted bilayer graphene [15]. Much effort has been devoted to reveal connections between the pairing in systems with spin, orbital, or nematic degrees of freedom [16–23]. Even the single-orbital square-lattice Hubbard model can be mapped to an effective multi-orbital system [24, 25], or we can explore non-Bravais lattices [26, 27], which provides novel perspectives and insights into the pairing mechanism. Often, the original or effective models exhibit wide and narrow bands, which raises the interesting question how the different bandwidths cooperate in the superconductivity.

Recently, it was shown that so-called incipient bands [26–32], which are full (empty) bands slightly below (above) the Fermi energy, can significantly enhance T_c. The concept of incipient bands was introduced by Kuroki *et al.* [26] in a fluctuation exchange (FLEX) [33] study of a Hubbard ladder. They found that the large number of interband pair-scattering channels promotes superconductivity. Linscheid *et al.* [34] argued that the incipient band contributes significantly to the spin-fluctuation pairing and leads to a high T_c in a two-band system with electron-like and hole-like bands. Very recently, Ochi *et al.* [32] studied a two-band continuum model with incipient narrow empty band with attractive interactions, and found that interband pair-hopping induces an effective intraband attraction in each band, enhancing superconductivity.

In the limit where the narrow band becomes flat, the normal-state kinetic energy of the electrons populating this band is quenched. Such (almost) flat bands appear in many van der Waals systems, including magic-angle twisted bilayer graphene [15] and its trilayer or double bilayer derivatives [35–38], and also in twisted bilayer WSe_2 [39] and MoS_2 [40]. This situation has been theoretically suggested to promote superconductivity for repulsive interactions [42]. While most previous works focused on models where either the narrow band or wide band is empty, we consider here a situation where *all bands are half-filled*. Based on the intuition from correlated systems in the normal state, one might expect that a flat band must be a Mott insulator (a paired Mott insulator in the case of attractive interactions that we consider here). However, we shall show that, when accompanied by a wide band, the flat band can be superconducting (SC) and that the exchange of pairs between the wide and flat bands results in a large SC order parameter in both bands.

Model and Method. We consider the Hubbard model on a bilayer square lattice with an attractive onsite interaction ($U < 0$),

$$H = \sum_{ij,ab} t_{ij}^{ab} c_{i,a\sigma}^{\dagger} c_{j,b\sigma} + U \sum_{ia} n_{i,a\uparrow} n_{i,a\downarrow}. \qquad (1)$$

Here a, b label the layers, and i, j the lattice sites, while $\sigma = \uparrow, \downarrow$ denotes the spin. The unit cell of the model contains two sites stacked along the z axis. The hopping parameters, depicted in Fig. 1, are the hopping t_1 for intra-layer nearest neighbors, t_2 for second neighbors, while the inter-layer hoppings are nearest-neighbor t_4 and second-neighbor t_3. The non-interacting Hamiltonian $H_0^{\uparrow}(\mathbf{k}) = H_0^{\downarrow}(\mathbf{k})$ is diagonal in the bonding-antibonding basis for cell i, $|i, {}^{\alpha}_{\beta}\sigma\rangle = (|i, a\sigma\rangle \pm |i, b\sigma\rangle)/\sqrt{2}$, with the bands $\epsilon_{{}^{\alpha}_{\beta},\mathbf{k}} = \pm t_4 + 4t_2 \cos k_x \cos k_y + 2(t_1 \pm t_3)(\cos k_x + \cos k_y)$. If $t_1 > 0$ and $t_3 > 0$, $\epsilon_\alpha(\mathbf{k})$ has a larger bandwidth than $\epsilon_\beta(\mathbf{k})$, see Fig. 1(c). When $t_2 = 0$ and $t_3 = t_1$, $\epsilon_\beta(\mathbf{k}) = -t_4$ is a flat band. The hopping t_4 deter-

* changming.yue@unifr.ch
† philipp.werner@unifr.ch

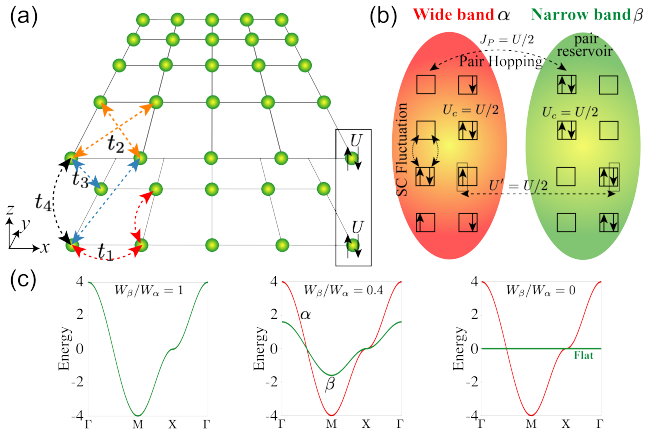


FIG. 1. (a) Bilayer square-lattice Hubbard model with sites depicted as green spheres and the two-site unit cell enclosed by a black box. t_1 (red) is the intra-layer hopping between nearest neighbor sites, while t_2 (orange) is for second-neighbor sites. t_4 (black) and t_3 (blue) are the inter-layer hoppings between nearest neighbor sites and next-nearest neighbor sites. (b) Schematic illustration showing the pair fluctuations (scatterings) within the wide band and between the two bands, as well as the relevant interactions. Black boxes in (b) represents unit-cells. (c) Non-interacting band structures for $W_\beta/W_\alpha = 1$, 0.4, 0.0, respectively.

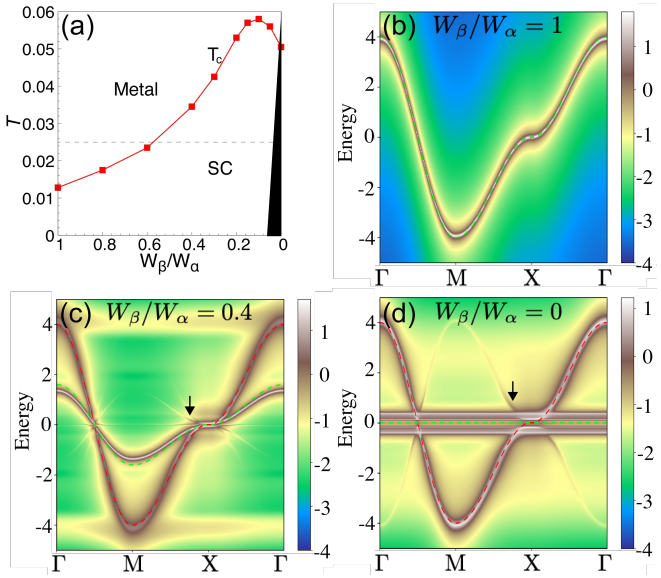


FIG. 2. (a) T_c versus the bandwidth ratio. The black region indicates the Mott phase in the flat band in the normal state. The Mott region extends to $W_\beta/W_\alpha \approx 0.05$ at $T = 0.01$. (b-d) Momentum-resolved spectral function $\log_{10}A(\mathbf{k},\omega)$ for the indicated values of W_β/W_α at $T = 0.025$ (horizontal dashed line in (a)). Here, the dashed lines show the non-interacting band structures. The black arrows in (c-d) highlight backbending of the Bogoliubov bands.

mines the energy splitting between the bonding and anti-bonding bands. Here we set $t_2 = t_4 = 0$ to have a particle-hole symmetry. The band width of each band is $W_{\substack{\alpha\\\beta}} = 8(t_1 \pm t_3)$. We fix the width of the wide band as $W_\alpha = 8$, and tune the narrow band width $W_\beta = 8(1-2t_3)$ by adjusting t_1 and t_3, and use $W_\alpha/8 = 1$ as energy unit.

The onsite Hubbard interaction can be transformed, within a unit cell i with two sites, into a two-orbital Hamiltonian,

$$\tilde{H}^i_{\rm int} = U_{\rm c}\sum_{\alpha} n_{i,\alpha\uparrow}n_{i,\alpha\downarrow} + U'\sum_{\alpha\neq\beta} n_{i,\alpha\uparrow}n_{i,\beta\downarrow} \qquad (2)$$
$$- J_P\sum_{\alpha\neq\beta} c^\dagger_{i,\alpha\uparrow}c^\dagger_{i,\alpha\downarrow}c_{i,\beta\uparrow}c_{i,\beta\downarrow} - J_S\sum_{\alpha\neq\beta} c^\dagger_{i,\alpha\uparrow}c_{i,\alpha\downarrow}c^\dagger_{i,\beta\downarrow}c_{i,\beta\uparrow},$$

with α (β) the bonding (anti-bonding) orbitals and $U_c = U' = J_P = J_S = U/2$ [24, 41, 42]. There is no inter-orbital same-spin interaction, since $U' - J_S = 0$. The J_P (J_S) term describes pair-hopping (spin-flipping) between the bonding and anti-bonding orbitals.

We solve the interacting lattice model using dynamical mean field theory (DMFT) [43], which maps the lattice problem to a self-consistently determined Anderson impurity model. To solve the two-orbital impurity model in the bonding/anti-bonding basis we employ the hybridization-expansion continuous-time quantum Monte Carlo algorithm [44–46]. We use four-operator updates to ensure an ergodic sampling in the SC phase [47]. Furthermore, we developed a normal (anomalous) worm-sampling to measure the normal (anomalous) Green's function for the flat band, since these functions cannot be measured with the conventional technique based on removing (anomalous) hybridization lines. Details on the anomalous worm algorithms are given in Sec. 5 of the Supplemental Material (SM), which includes Ref. [49–52]. In the Nambu-formalism, the non-interacting lattice Hamiltonian reads

$$H_0 = \sum_{\boldsymbol{k}}\begin{bmatrix}\Psi^\dagger_{\boldsymbol{k},\uparrow} & \Psi_{-\boldsymbol{k},\downarrow}\end{bmatrix}\begin{bmatrix}H_0^\uparrow(\mathbf{k}) & 0\\ 0 & -H_0^\downarrow(-\mathbf{k})^T\end{bmatrix}\begin{bmatrix}\Psi_{\boldsymbol{k},\uparrow}\\ \Psi^\dagger_{-\boldsymbol{k},\downarrow}\end{bmatrix},$$

where we define the Nambu spinors $[\,\Psi^\dagger_{\boldsymbol{k},\uparrow}\;\;\Psi_{-\boldsymbol{k},\downarrow}\,] = [\,c^\dagger_{\mathbf{k},\alpha\uparrow},\; c^\dagger_{\mathbf{k},\beta\uparrow},\; c_{-\mathbf{k},\alpha\downarrow},\; c_{-\mathbf{k},\beta\downarrow}\,]$. The interacting lattice Green's function can be expressed as

$$G(\mathbf{k}, i\omega_n) = [i\omega_n\mathbb{I}_4 + \sigma_3\otimes\mu\mathbb{I}_2 - H_0(\mathbf{k}) - \Sigma^{\rm Nambu}(i\omega_n)\mathbb{I}_4]^{-1},$$

where $\Sigma^{\rm Nambu}$ is the local self-energy from DMFT. Unless otherwise mentioned, we set $U = -1$ and $\mu = U/2$ to make the system particle-hole symmetric.

Phase diagram and quasi-particle spectra. Figure 2(a) presents the DMFT phase diagram in the space of temperature T and bandwidth ratio W_β/W_α. Both bands become superconducting simultaneously and we determine T_c by extrapolating the square-root like critical behavior of the SC order parameter (see SM Sec. 3). The red line shows T_c against W_β/W_α. For $W_\beta/W_\alpha = 1$, we have $T_c \simeq 0.0128$. In this limit with $t_3 = 0$ the two layers are decoupled, so that the system decomposes into two independent single-band Hubbard models on the square lattice. As one decreases W_β/W_α from 1,

T_c is seen to increase. This can be understood by the decreasing width of the narrow band, where $|U|/W_\beta$ increases, i.e., T_c increases with increasing electron correlations. For $W_\beta/W_\alpha \lesssim 0.4$, T_c markedly increases with decreasing bandwidth ratio and reaches its maximum value of 0.058 (nearly 5 times the T_c at $W_\beta/W_\alpha = 1$) around $W_\beta/W_\alpha \simeq 0.1$. Then T_c drops slightly as one further decreases W_β/W_α from 0.1 to 0, but it remains high even when the non-interacting anti-bonding band becomes flat. In particular, T_c for the coupled bilayer system with $W_\alpha = 8$, $W_\beta = 0$ is much higher than for the decoupled layers with $W_\alpha = W_\beta = 8$.

We now look at the momentum-resolved spectral function, obtained from the Nambu Green's functions as $A(\mathbf{k},\omega) = -\frac{2}{\pi}\mathrm{Im}[G_{1\uparrow,1\uparrow} + G_{2\uparrow,2\uparrow}](\mathbf{k},\omega)$. For the analytic continuation from the Matsubara to the real-frequency axis, we use the auxiliary [48] maximum entropy [49] method, where the real-frequency self-energy $\Sigma(\omega)$ is constructed from two auxiliary self-energy functions $\Sigma_\pm = \Sigma^{\mathrm{nor}} \pm \Sigma^{\mathrm{ano}}$ which have positive definite spectral weight in the presence of particle-hole symmetry [53]. Figure 2(b-d) shows the spectra for $W_\beta/W_\alpha = 1$, 0.4 and 0 at $T = 0.025$. For comparison, we overlay the corresponding non-interacting bands. The system becomes SC for $W_\beta/W_\alpha \lesssim 0.57$ at $T = 0.025$, as shown in Fig. 2(a), and therefore a SC gap opens in both bands in panels (c,d). There the black arrow marks the back-bending of the Bogoliubov bands, which demonstrates particle-hole mixing, a fundamental consequence of pair condensation [54, 55]. At $W_\beta = 0$, the narrow band becomes flat but remains superconducting. The spectral functions in the normal and SC state are compared in detail in SM Sec. 2. There it is shown that in the SC state, the gap in the wide band is a SC gap, while the gap in the flat band has two contributions and can be interpreted as a Mott gap enhanced by the SC gap.

Order parameter and phase stiffness. The phase stiffness D_S measures the rigidity of the SC state against phase twisting. We calculate D_S in the framework of linear response and in the long-wave-length limit, following Refs. 23, 56, and 57 as $D_{S,xx} = D^{\mathrm{par}}_{S,xx} + D^{\mathrm{dia}}_{S,xx}$ with $D^{\mathrm{par}}_{S,xx} = \frac{e^2T}{\hbar^2VN}\sum_{\mathbf{k},i\omega_n} \mathrm{Tr}G(\mathbf{k},i\omega_n)(\sigma_0 \otimes \lambda^x_{\mathbf{k}})G(\mathbf{k},i\omega_n)(\sigma_0 \otimes \lambda^x_{\mathbf{k}})$ and $D^{\mathrm{dia}}_{S,xx} = \frac{e^2T}{\hbar^2VN}\sum_{\mathbf{k},i\omega_n} \mathrm{Tr}G(\mathbf{k},i\omega_n)e^{i\omega_n 0^+}(\sigma_3 \otimes \lambda^{xx}_{\mathbf{k}})$, where $\lambda^x_{\mathbf{k}} \equiv \partial_{\mathbf{k}_x}H_0(\mathbf{k})$, and $\lambda^{xx}_{\mathbf{k}} \equiv \partial^2_{\mathbf{k}_x}H_0(\mathbf{k})$. A mesh of 395×395 $\mathbf{k}$-points is used to calculate the stiffness. The orbital-resolved order parameters $\Delta_\alpha = \langle c_{\alpha\uparrow}c_{\alpha\downarrow}\rangle$ and $\Delta_\beta = \langle c_{\beta\uparrow}c_{\beta\downarrow}\rangle$, and corresponding stiffnesses $D^\alpha_{S,xx}$ and $D^\beta_{S,xx}$ ($D^\alpha_{S,xx} + D^\beta_{S,xx} = D_{S,xx}$) are plotted against W_β/W_α in Fig. 3 by the blue lines. Panels (a,c) show the results for the wide band and panels (b,d) those for the narrow band. We set $T = 0.025$, so that the model becomes SC for $W_\beta/W_\alpha \lesssim 0.57$. The order parameter and stiffness in the wide band increase with decreasing W_β and reach respective maxima in or near the flat-band limit $W_\beta = 0$. This shows that the stronger correlations in the narrow band and the enhanced interband

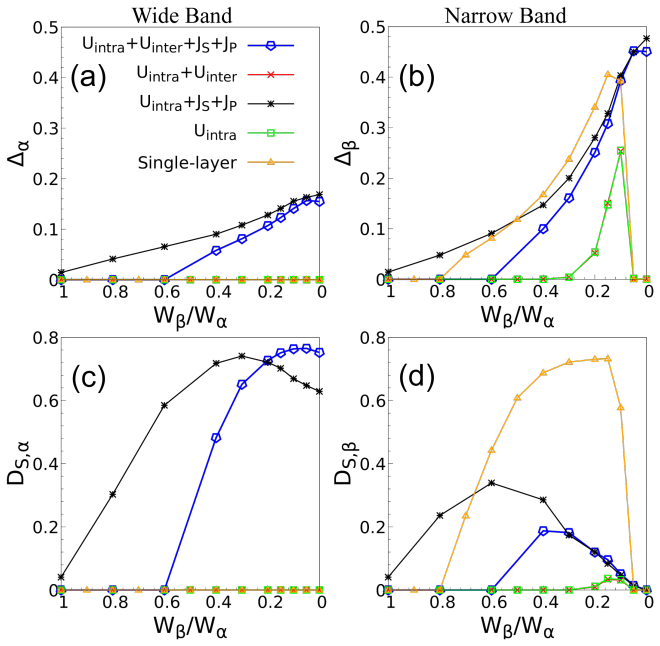


FIG. 3. (a,b) SC order parameter Δ and (c,d) superfluid stiffness D_S (in units of $e^2/\hbar^2$) in the two bands against W_β/W_α at $T = 0.025$. Panels (a,c) are for the wide band (α) and panels (b,d) for the narrow band (β). Green symbols: results when only intra-orbital interactions are considered; red: for intra-orbital plus inter-orbital density-density interactions; black: for intra-orbital interactions plus spin-flip and pair-hopping terms; blue: for the full model. Orange symbols in (b,d) [(a,c)] : results for a single-band model with varying bandwidth $W = W_\beta$ [fixed bandwidth $W = W_\alpha = 8$].

pairing interactions boost superconductivity in the wide band. Note that a single-band model with bandwidth 8 and $U = -1$ would not be superconducting at this temperature (orange curves in panels (a,c)).

In the narrow band, while the order parameter shows a stronger increase reaching its maximum near $W_\beta = 0$, the stiffness exhibits a much less pronounced increase than in the wide band, followed by a decrease as the narrow band enters into the strong-correlation regime. Remarkably, the narrow band does *not* become a paired Mott insulator for small W_β unlike in the single-band model (orange curves in panels (b,d)), see also the spectra in SM Sec. 4. This shows that the superconductivity in the narrow band is supported by the interactions with the wide band in the strong-correlation regime.

To analyze the mechanism behind the enhancement of superconductivity in the narrow band, let us resolve the effects of the different interaction terms in the effective two-orbital Hamiltonian (2) by turning them on term by term. The green lines in Fig. 3 show the results obtained when we only retain the intra-orbital interaction U_c, i.e., for a system without any coupling between the bonding and anti-bonding orbitals. In this case, the only relevant quantities are the ratios U_c/W_α and U_c/W_β. Since we decrease W_β at fixed W_α, we see the behavior expected

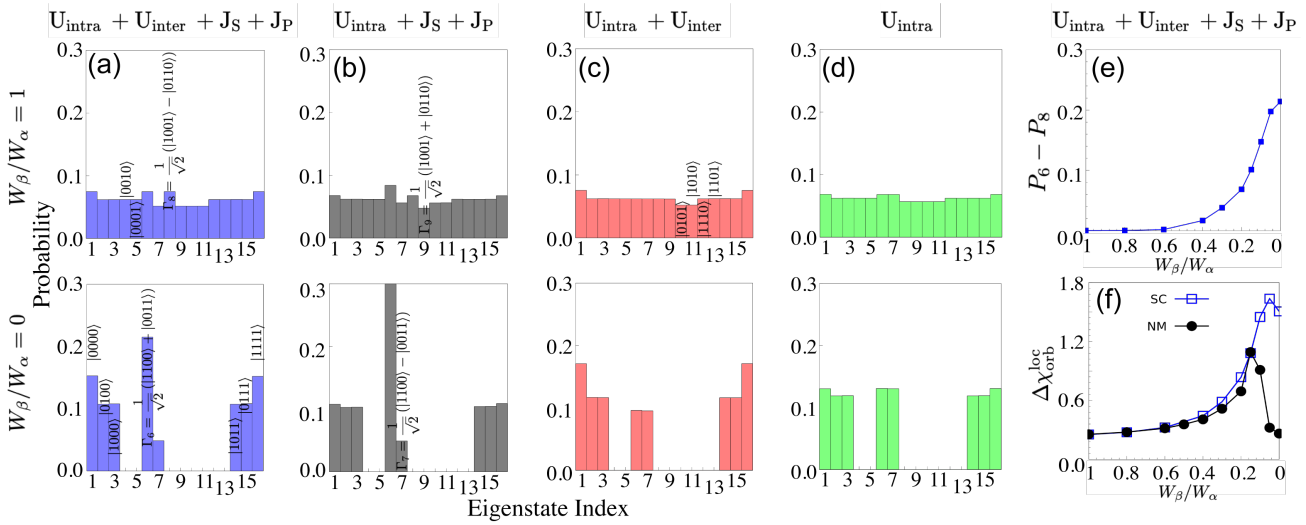


FIG. 4. (a-d) DMFT histograms of atomic eigenstates for models with different interaction terms. Results are shown for the model with (a) all the interaction terms, (b) the U_c, J_S, J_P terms, (c) the U_c, U' terms, and (d) the U_c term only. The top (bottom) row is for $W_\beta/W_\alpha = 1$ (0) in (a-d). (e) Difference in probabilities $P_{\Gamma_6} - P_{\Gamma_8}$ as a function of W_β/W_α in the full model. (f) Dynamic contribution to the local orbital susceptibility for the full model in the SC and normal metal (NM) phase. The temperature is $T = 0.025$.

for the single-band attractive Hubbard model: the order parameter in the wide band remains constant, while it increases in the narrow band, up to the Mott transition point at $W_\beta/W_\alpha \simeq 0.1$ (see spectra of the U_c model in SM Sec. 4). When we add the inter-orbital interactions U' to the intra-orbital interactions U_c we obtain similar results as shown by the red lines in Fig. 3, which overlap with the green lines (the almost negligible effect of U' is because of the small value of $U = -1$).

If instead we consider U_c and the pair-hopping and spin-flip terms (black lines in Fig. 3), the results are remarkably different. The order parameters in both bands are now larger than for the full model, especially for W_β/W_α near 1, and they increase monotonically with decreasing W_β. Also the stiffness is strongly enhanced for $W_\beta/W_\alpha \gtrsim 0.4$. Since we are considering here intra-orbital pairing, it is natural to assume that the pair-hopping (rather than spin-flip) term is the relevant player in the observed enhancement of superconductivity.

To further analyze the interplay between the interaction terms, we look at the probability weights of the 16 eigenstates of $\tilde{H}^i_{\rm int}$ (Eq. (2)) [58], measured with DMFT. Panels (a-d) in Fig. 4 show them for $W_\beta/W_\alpha = 1$ (top) and $W_\beta/W_\alpha = 0$ (bottom), for the four types of interactions with the same color code as in Fig. 3. We label the eigenstates Γ using a binary code of the occupation status per spin-orbital $|n_{\alpha\uparrow}n_{\alpha\downarrow}n_{\beta\uparrow}n_{\beta\downarrow}\rangle$ as indicated in the figure. In panel (a) we see that, for $W_\beta/W_\alpha = 1$, the eigenstate $\Gamma_6 \equiv \frac{1}{\sqrt{2}}(|1100\rangle + |0011\rangle)$ of the pair-hopping term $H_P = -J_P \sum_{\alpha\neq\beta} c^\dagger_{i,\alpha\uparrow}c^\dagger_{i,\alpha\downarrow}c_{i,\beta\uparrow}c_{i,\beta\downarrow}$ is as important as the eigenstate $\Gamma_8 = \frac{1}{\sqrt{2}}(|1001\rangle - |0110\rangle)$ of the spin-flip term $H_S = -J_S \sum_{\alpha\neq\beta} c^\dagger_{i,\alpha\uparrow}c_{i,\alpha\downarrow}c^\dagger_{i,\beta\downarrow}c_{i,\beta\uparrow}$, while for $W_\beta/W_\alpha = 0$, Γ_6, with a combination of inter-band pair-hopped states, clearly dominates. In the model without the U' term (panel (b)), Γ_6 is already more relevant than Γ_8 at $W_\beta/W_\alpha = 1$ and it completely dominates for $W_\beta/W_\alpha = 0$.

The pair hopping term boosts superconductivity, as seen from Δ in Fig. 3, as long as the pairs have a large phase stiffness (are sufficiently delocalized). A too dominant Γ_6 state, as in the case of $W_\beta/W_\alpha \approx 0$ in the model without U', weakens the superfluid stiffness (Fig. 3(c)). The suppression of Δ and D_S in the full model with $W_\beta/W_\alpha = 1$, compared to the model without U', can be explained from the setting $U_c = U' = J_S = J_P$. The density-density interaction is the same for intra-orbital and inter-orbital opposite-spin pairs, so that both the pair-hopping and spin-flipping terms are active and stabilize the states Γ_6 and Γ_8, respectively. Γ_8 however favors inter-orbital pairing and suppresses intra-orbital pairing, which explains the smaller order parameter and lower T_c of the full model with $W_\beta/W_\alpha = 1$. For $W_\beta/W_\alpha < 1$ the symmetry between the bonding and antibonding orbitals is broken and the intra-orbital correlations in the narrow band start to dominate the inter-orbital correlations. This leads to a strongly correlated metal with a high probability of doublons and holons in the narrow band of this attractive-U system, and suppresses the Γ_8 states. The result is the strong increase in Δ seen in Fig. 3(a,b) (blue line). Meanwhile, the presence of the U' interaction prevents too strong a dominance of the Γ_6 state by favoring the full (Γ_{16}) and empty (Γ_1) states. Hence the full model with pair-hopping and U' favors, for small enough W_β, a state which supports pair fluctuations and exhibits a large stiffness (blue line in Fig. 3(c)). We can think of the flat band as a reservoir of pairs,

which are injected into the wide band via pair-hopping processes, thus boosting superconductivity in the wide band. At the same time, the pair-hopping enables a kind of proximity effect [60], which allows the narrow band to remain superconducting even in the flat-band limit. To support the relevance of this mechanism, we plot in Fig. 4(e) the difference $P_6 - P_8$ between the probabilities of Γ_6 and Γ_8. The strong upturn around $W_\beta/W_\alpha \approx 0.4$ is qualitatively similar to the increase seen in $\Delta_{\alpha,\beta}$.

A second factor that plays a role in the pairing is the enhancement of the attractive interactions through local moment fluctuations. For a weak enough bare interaction, this effect can be captured by calculating an effective screened interaction which takes into account bubble diagrams, as demonstrated in several works [19, 61–64]. Within the random phase approximation, the effective static interactions are given as $\tilde{J}_{P,S} = (U/2)/[1 - \frac{U}{2}(\chi^{\uparrow\uparrow}_{1212} + \chi^{\uparrow\uparrow}_{2121})\frac{U}{2}(\chi^{\downarrow\downarrow}_{1212} + \chi^{\downarrow\downarrow}_{2121})]$ and $\tilde{U}_c, \tilde{U}' = (U/2)/[1 - \frac{U}{2}(\chi^{\uparrow\uparrow}_{1111} + \chi^{\uparrow\uparrow}_{2222})\frac{U}{2}(\chi^{\downarrow\downarrow}_{1111} + \chi^{\downarrow\downarrow}_{2222})]$, where $\chi^{\sigma\sigma}_{pqst}(\Omega = 0) = -T\sum_m G^{\sigma}_{ps}(i\omega_m)G^{\sigma}_{tq}(i\omega_m)$. In the weak-coupling limit, all the effective interactions are enhanced by the third-order term in U, and this effect is augmented in the narrow-band regime if χ itself increases with decreasing W_β. In the density sector, χ is related to the orbital susceptibility $\chi_{\rm orb}$ [64]. Since the orbital moments in our effective two-orbital model can freeze in the strong-correlation regime [63], we replace $\chi^{\rm orb}_{\rm loc}(\Omega = 0)$ with the fluctuation contribution to the DMFT orbital correlation function, $\Delta\chi^{\rm orb}_{\rm loc} = \int_0^\beta d\tau \chi^{\rm orb}_{\rm loc}(\tau) - \beta\chi^{\rm orb}_{\rm loc}(\beta/2)$. As shown in Fig. 4(f), $\Delta\chi^{\rm orb}_{\rm loc}$ in the normal phase (circles) grows with decreasing W_β/W_α, and reaches its maximum around $W_\beta/W_\alpha = 0.16$ before the narrow band becomes Mott insulating and the local orbital moments freeze. The orbital-frozen metal state has a large entropy [64, 65], which is released if the system goes into a SC phase. In the SC phase (empty squares in panel (f)), $\Delta\chi^{\rm orb}_{\rm loc}$ continues to increase sharply with decreasing W_β/W_α reaching a maximum closer to the flat-band limit. The feedback of the enhanced orbital fluctuations on the effective attraction contributes to the boosting of T_c in the narrow- and flat-band regimes. The dip in $\Delta\chi^{\rm loc}_{\rm orb}$ near $W_\beta = 0$ may explain the similar dip seen in T_c (red curve in Fig. 2(a)).

So far we have employed the bonding/anti-bonding basis, but we can readily translate the SC order parameters back to the original site basis. Since $c_{\substack{\alpha\\\beta}\uparrow}c_{\substack{\alpha\\\beta}\downarrow} = \frac{1}{2}(c_{a\uparrow} \pm c_{b\uparrow})(c_{a\downarrow} \pm c_{b\downarrow}) = \frac{1}{2}(c_{a\uparrow}c_{a\downarrow} + c_{b\uparrow}c_{b\downarrow} \pm c_{a\uparrow}c_{b\downarrow} \pm c_{b\uparrow}c_{a\downarrow})$, with a, b labeling the layers, and $\Delta_\beta > \Delta_\alpha$ for $W_\beta/W_\alpha < 1$, one generically finds that $\Delta_{aa} = \Delta_{bb} = \frac{1}{2}(\Delta_\alpha + \Delta_\beta)$ and $\Delta_{ab} = \Delta_{ba} = \frac{1}{2}(\Delta_\alpha - \Delta_\beta) \neq 0$. The system with $W_\beta = 0$ exhibits both local pairing with amplitude $\frac{1}{2}(\Delta_\alpha + \Delta_\beta)$ and inter-layer spin-singlet pairing $\langle c_{a\uparrow}c_{b\downarrow} - c_{a\downarrow}c_{b\uparrow}\rangle = \frac{1}{2}(\Delta_\alpha - \Delta_\beta)$. At $W_\beta/W_\alpha = 1$, we have instead $\Delta_{aa} = \Delta_{bb} = \Delta_\alpha = \Delta_\beta$ with $\Delta_{ab} = \Delta_{ba} = 0$, and thus only intra-site pairing, as expected for decoupled layers.

Conclusions. We have demonstrated significant enhancements of superconductivity associated with the interplay between wide and narrow bands. In a half-filled and particle-hole symmetric system with attractive interactions, the strong correlations in the narrow or flat band favor doublons and holons, whose injection into and interaction with the wide band boosts the superfluid stiffness and T_c. By a kind of proximity effect (pair-hopping term in the bonding/antibonding basis), the superconductivity in the wide band supports the superconductivity in the narrow band even in the flat-band limit. The pairing is additionally boosted by local orbital fluctuations which effectively enhance the attractive interactions.

Our results are not related to topological effects [66, 67], since the bandstructure of the bilayer system is non-topological and the wide band features no gap. The findings are also qualitatively different from the previous results related to incipient bands [26–32], since these works considered the effects of full or empty narrow bands in repulsive models and found that the half-filled situation does not favor superconductivity [29]. Our bandstructure and the bonding/antibonding transformation used to study the interaction effects is related to previous analyses of the square lattice Hubbard model [24] and diamond chain [27]. It will be interesting to extend the results of this study to repulsive systems by investigating the role of narrow bands as a reservoir or seed of local moments, and to clarify the effects on superconductivity induced by local moment fluctuations.

Acknowledgements. — The calculations were performed on the Beo05 cluster at the University of Fribourg, using a code based on iQIST [68, 69]. C.Y. and P.W. acknowledge support from SNSF Grant No. 200021-196966. H.A. thanks CREST (Core Research for Evolutional Science and Technology project from Japan Science and Technology Agency; Grant Number JPMJCR18T4).

[1] G. R. Stewart, Rev. Mod. Phys. **83,** 1589 (2008).
[2] Y. Kamihara, H. Hiramatsu, M. Hirano, R. Kawamura, H. Yanagi, T. Kamiya, and H. Hosono, J. Am. Chem. Soc. **128**, 10012 (2006).
[3] Y. Kamilhara, T. Watanabe, M. Hirano, and H. Hosono, J. Am. Chem. Soc. **130**, 3296 (2008).
[4] X. C. Wang, Q. Q. Liu, Y. X. Lv, W. B. Gao, L. X. Yang, R. C. Yu, F. Y. Li, and C. Q. Jin, Solid State Commun. **148**, 538 (2008).
[5] M. Rotter, M. Tegel, and D. Johrendt, Phys. Rev. Lett. **101**, 107006 (2008).
[6] P. M. Shirage, K. Miyazawa, H. Kito, H. Eisaki and A. Iyo, Appl. Phys. Express **1**, 081702 (2008).
[7] K. Sasmal, B. Lv, B. Lorenz, A. M. Guloy, F. Chen, Y.-Y. Xue, and C.-W. Chu, Phys. Rev. Lett. **101**, 107007 (2008).

[8] C. W. Chu, F. Chen, M. Gooch, A. M. Guloy, B. Lorenz, B. Lv, K. Sasmal, Z. J. Tang, J. H. Tapp, and Y. Y. Xue, Physica C: Superconductivity, **469**, 326 (2009).

[9] Q.-Y. Wang, Z. Li, W.-H. Zhang, Z.-C. Zhang, J.-S. Zhang, W. Li, H. Ding, Y.-B. Ou, P. Deng, K. Chang, J. Wen, C.-L. Song, K. He, J.-F. Jia, S.-H. Ji, Y.-Y. Wang, L.-L. Wang, X. Chen, X.-C. Ma, and Q.-K. Xue, Chin. Phys. Lett. **29**, 037402 (2012).

[10] D. Liu, W. Zhang, D. Mou, J. He, Y.-B. Ou, Q.-Y. Wang, Z. Li, L. Wang, L. Zhao, S. He, Y. Peng, X. Liu, C. Chen, L. Yu, G. Liu, X. Dong, J. Zhang, C. Chen, Z. Xu, and J. Hu et al., Nat. Commun. **3**, 931 (2012).

[11] S. He, J. He, W. Zhang, L. Zhao, D. Liu, X. Liu, D. Mou, Y.-B. Ou, Q.-Y. Wang, Z. Li, L. Wang, Y. Peng, Y. Liu, C. Chen, L. Yu, G. Liu, X. Dong, J. Zhang, C. Chen, and Z. Xu et al., Nat. Mater. **12**, 605 (2013).

[12] S. Tan, Y. Zhang, M. Xia, Z. Ye, F. Chen, X. Xie, R. Peng, D. Xu, Q. Fan, H. Xu, J. Jiang, T. Zhang, X. Lai, T. Xiang, J. Hu, B. Xie, and D. Feng, Nat. Mater. **12**, 634 (2013).

[13] W.-H. Zhang, Y. Sun, J.-S. Zhang, F.-S. Li, M.-H. Guo, Y.-F. Zhao, H.-M. Zhang, J.-P. Peng, Y. Xing, H.-C. Wang, T. Fujita, A. Hirata, Z. Li, H. Ding, C.-J. Tang, M. Wang, Q.-Y. Wang, K. He, S.-H. Ji, X. Chen, J.-F. Wang, Z.-C. Xia, L. Li, Y.-Y. Wang, J. Wang, L.-L. Wang, M.-W. Chen, Q.-K. Xue, and X.-C. Ma, Chin. Phys. Lett. **31**, 017401 (2014).

[14] Y. Zhang, J. J. Lee, R. G. Moore, W. Li, M. Yi, M. Hashimoto, D. H. Lu, T. P. Devereaux, D.-H. Lee, and Z.-X. Shen, Phys. Rev. Lett. **117**, 117001 (2016).

[15] Y. Cao, V. Fatemi, S. Fang, K. Watanabe, T. Taniguchi, E. Kaxiras, and P. Jarillo-Herrero, Nature (London) **556**, 43 (2018).

[16] Kazuhiko Kuroki, Seiichiro Onari, Ryotaro Arita, Hidetomo Usui, Yukio Tanaka, Hiroshi Kontani, and Hideo Aoki, Phys. Rev. Lett. **101,** 087004 (2008).

[17] H. Kontani and S. Onari, Phys. Rev. Lett. **104**, 157001 (2010).

[18] A. Chubukov, Annu. Rev. Condens. Matter Phys. **3**, 57 (2012).

[19] S. Hoshino, and P. Werner, Phys. Rev. Lett. **115**, 247001 (2015).

[20] Zi-Xiang Li, Fa Wang, Hong Yao and Dung-Hai Lee, Science Bulletin **61**, 925 (2016).

[21] P. T. Dumitrescu, M. Serbyn, R. T. Scalettar, and A. Vishwanath, Phys. Rev. B **94**, 155127 (2016).

[22] D. Huang and J. E. Hoffman, Annu. Rev. Condens. Matter Phys. **8**, 311 (2017).

[23] C. Yue and P. Werner, Phys. Rev. B **104**, 184507 (2021).

[24] P. Werner, S. Hoshino, and H. Shinaoka, Phys. Rev. B **94**, 245134 (2016).

[25] P. Werner, X. Chen, and E. Gull, Phys. Rev. Research **2**, 023037 (2020).

[26] K. Kuroki, T. Higashida, and R. Arita, Phys. Rev. B **72,** 212509 (2005).

[27] K. Kobayashi, M. Okumura, S. Yamada, M. Machida, and H. Aoki, Phys. Rev. B **94**, 214501 (2016).

[28] X. Chen, S. Maiti, A. Linscheid, and P. J. Hirschfeld, Phys. Rev. B **92,** 224514 (2015).

[29] K. Matsumoto, D. Ogura, and K. Kuroki, J. Phys. Soc. Jpn. **89**, 044709 (2020).

[30] D. Kato and K. Kuroki, Phys. Rev. Research **2**, 023156 (2020).

[31] S. Karakuzu, S. Johnston, and T. A. Maier, Phys. Rev. B **104**, 245109 (2021).

[32] K. Ochi, H. Tajima, K. Iida, and H. Aoki, Phys. Rev. Research **4**, 013032 (2022).

[33] N. E. Bickers, D. J. Scalapino, and S. R. White, Phys. Rev. Lett. **62,** 961 (1989).

[34] A. Linscheid, S. Maiti, Y. Wang, S. Johnston, and P. J. Hirschfeld, Phys. Rev. Lett. **117,** 077003 (2015)

[35] C. Shen, Y. Chu, Q. Wu, N. Li, S. Wang, Y. Zhao, J. Tang, J. Liu, J. Tian, K. Watanabe, T. Taniguchi, R. Yang, Z. Y. Meng, D. Shi, O. V. Yazyev, and G. Zhang,Nat. Phys. **16,** 520 (2020)

[36] Y. Cao, D. Rodan-Legrain, O. Rubies-Bigorda, J. M. Park, K. Watanabe, T. Taniguchi, and P. Jarillo-Herrero, Nature **583**, 215 (2020).

[37] X. Liu, Z. Hao, E. Khalaf, J. Y. Lee, Y. Ronen, H. Yoo, D. H. Najafabadi, K. Watanabe, T. Taniguchi, A. Vishwanath, and P. Kim, Nature (London) **583**, 221 (2020).

[38] Xi Zhang, Kan-Ting Tsai, Ziyan Zhu, Wei Ren, Yujie Luo, Stephen Carr, Mitchell Luskin, Efthimios Kaxiras, and Ke Wang, Phys. Rev. Lett. **127**, 2021 (166802).

[39] L. Wang, E.-M. Shih, A. Ghiotto, L. Xian, D. A. Rhodes, C. Tan, M. Claassen, D. M. Kennes, Y. Bai, B. Kim, K. Watanabe, T. Taniguchi, X. Zhu, J. Hone, A. Rubio, A. N. Pasupathy, and C. R. Dean, Nat. Mater. **19**, 861 (2020).

[40] L. Xian, M. Claassen, D. Kiese, M. Scherer, S. Trebst , D. M. Kennes, and A. Rubio, Nat. Commun. **12**, 5644 (2021).

[41] H. Shinaoka, Y. Nomura, S. Biermann, M. Troyer, and P. Werner, Phys. Rev. B **92**, 195126 (2015).

[42] H. Aoki, J. Superconductivity and Novel Magnetism **33**, 2341 (2020).

[43] A. Georges, G. Kotliar, W. Krauth, and M. J. Rozenberg, Rev. Mod. Phys. **68**, 13 (1996).

[44] P. Werner, A. Comanac, L. de' Medici, M. Troyer, and A. J. Millis, Phys. Rev. Lett. **97**, 076405 (2006).

[45] P. Werner and A. J. Millis, Phys. Rev. B **74,** 155107 (2006).

[46] E. Gull, A. J. Millis, A. I. Lichtenstein, A. N. Rubtsov, M. Troyer, and P. Werner, Rev. Mod. Phys. **83**, 349 (2011).

[47] P. Sémon, G. Sordi, A.-M. S. Tremblay, Phys. Rev. B **89**, 165113 (2014).

[48] A. Reymbaut, D. Bergeron, and A. M. S. Tremblay, Phys. Rev. B **92**, 060509(R) (2015).

[49] M. Jarrell and J. Gubernatis, Phys. Rep. **269**, 133 (1996).

[50] P. Gunacker, M. Wallerberger, E. Gull, A. Hausoel, G. Sangiovanni, and K. Held, Phys. Rev. B. **92,** 155102 (2015).

[51] P. Gunacker, M. Wallerberger, T. Ribic, A. Hausoel, G. Sangiovanni, and K. Held, Phys. Rev. B. **94,** 125153 (2015).

[52] L. M. Falicov and J. C. Kimball, Phys. Rev. Lett. **22,** 997 (1969).

[53] E. Gull, O. Parcollet, and A. J. Millis, Phys. Rev. Lett. **110**, 216405 (2013).

[54] J. R. Schrieffer, Theory of Superconductivity W. A. Benjamin, New York (1964).

[55] J. C. Campuzano, H. Ding, M. R. Norman, M. Randeira, A. F. Bellman, T. Yokoya, T. Takahashi, H. Katayama-Yoshida, T. Mochiku, and K. Kadowaki, Phys. Rev. B **53**, 14737(R) (1996).

[56] O. Simard, C.-D. Hébert, A. Foley, D. Sénéchal, and A.-M. S. Tremblay, Phys. Rev. B **100**, 094506 (2019).

[57] P. Coleman, Introduction to Many-Body Physics, Cam-

bridge University Press (2015).
[58] See Supplemental Material for the eigenstates and eigenvalues of the different local Hamiltonians, and for simulation results at lower temperature.
[59] A. Toschi, M. Capone, and C. Castellani, Phys. Rev. B **72**, 235118 (2005).
[60] In the usual proximity effect, a metal next to a SC becomes itself SC because of pairs leaking into the normal region. Here we have a SC state in the wide band which "leaks" pairs into the narrow band though pair hopping.
[61] K. Inaba and S.-i. Suga, Phys. Rev. Lett. **108**, 255301 (2012).
[62] S. Hoshino, and P. Werner, Phys. Rev. Lett. **118**, 177002 (2017).
[63] K. Steiner, S. Hoshino, Y. Nomura, and P. Werner, Phys. Rev. B **94**, 075107 (2016).
[64] C. Yue, S. Hoshino, A. Koga, and P. Werner, Phys. Rev. B **104**, 075107 (2021).
[65] C. Yue, and P. Werner, Phys. Rev. B **102**, 085102 (2020).
[66] S. Peotta and Päivi Törmä, Nature Comm. **6**, 8944 (2015).
[67] N. Verma, T. Hazra, and M. Randeria, Proc. National Academy of Sciences **118**, e2106744118 (2021).
[68] L. Huang, Y. Wang, Z. Y. Meng, L. Du, P. Werner, and X. Dai, Comput. Phys. Commun **195**, 140 (2015).
[69] L. Huang, Comput. Phys. Commun **221**, 423 (2017).